

## Understanding the Mechanism of Gelation and Stimuli-Responsive Nature of a Class of Metallo-Supramolecular Gels

Wengui Weng, J. Benjamin Beck, Alex M. Jamieson,\* and Stuart J. Rowan\*

Contribution from the Department of Macromolecular Science & Engineering, Case Western Reserve University, Cleveland, Ohio 44106

Received May 16, 2006; E-mail: stuart.rowan@case.edu; alex.jamieson@case.edu

**Abstract:** Utilizing metal–ligand binding as the driving force for self-assembly of a ditopic ligand, which consists of a 2,6-bis-(1'-methylbenzimidazolyl)-4-oxypyridine moiety attached to either end of a penta-(ethylene glycol) core, in the presence of a transition metal ion ( $Zn^{II}$ ) and a lanthanide metal ion ( $La^{III}$ ), we have achieved formation of stimuli-responsive metallo-supramolecular gels. We describe herein a series of experimental studies, including optical and confocal microscopy, dynamic light scattering, wide-angle X-ray diffraction, and rheology, to explore the properties of such gels, as well as the nature of the gelation mechanism. Morphological and X-ray diffraction observations suggest gelation occurs via the flocculation of semicrystalline colloidal particles, which results in the gels exhibiting pronounced yielding and thixotropic behavior. Application of mechanical stress results in a decrease in the particle size, which is accompanied by an increase in gel strength after removal of the stress. Moreover, studies show that the presence of lanthanide(III) perchlorate increases the mechano-responsiveness of the gels, as a consequence of reduced crystallinity of the colloidal particles, presumably due to the different coordination ability of lanthanide(III) and zinc(II), which changes the nature of the self-assembly in these materials.

### Introduction

Stimuli-responsive polymers, which are a class of “smart” materials,<sup>1</sup> exhibit a dramatic change in their properties in response to the application of an environmental stimulus, such as temperature, ionic strength, pH, solvent polarity, electric or magnetic fields, biological and chemical analytes, etc. According to the kind of stimulus that they respond to, such materials can be classified into photo-, chemo-, electro-, mechano-active polymers, etc. Examples include liquid crystal polymers,<sup>2</sup> polymer solutions and gels capable of undergoing phase transition,<sup>3</sup> electro- and magnetorheological fluids,<sup>4,5</sup> and electro-active polymers (EAPs).<sup>6</sup> Polymers of this type are being developed for potential uses in fields as diverse as bulk engineering and microscale medicine, while specific examples

range from smart films,<sup>7,8</sup> sensors,<sup>9,10</sup> electro-optic devices,<sup>11</sup> microfluidic devices,<sup>12</sup> pulsatile drug release systems,<sup>13</sup> bioadhesion mediators,<sup>14</sup> and actuators,<sup>15,16</sup> etc.

Supramolecular chemistry, which utilizes reversible noncovalent interactions, has been applied by a number of groups in recent years to bind monomeric units together into larger structures and polymeric aggregates.<sup>17</sup> The properties of such self-assembled polymers will depend on factors such as degree of polymerization (DP), architecture (e.g., linear or branched), and the dynamics/lifetime of the aggregate, which can be

- (1) (a) Yerushalmi, R.; Scherz, A.; van der Boom, M. E.; Kraatz, H.-B. *J. Mater. Chem.* **2005**, *15*, 4480–4487. (b) Nath, N.; Chilkoti, A. *Adv. Mater.* **2002**, *14*, 1243–1247. (c) *Multilayer Thin Films*; Decher, G., Schlenoff, J. B., Eds.; Wiley-VCH Verlag GmbH: Weinheim, 2003. (d) *Stimuli-Responsive Water Soluble and Amphiphilic Polymers*; McCormick, C. L., Ed.; ACS Symposium Series 780; American Chemical Society: Washington, DC, 2001. (e) de las Heras Alarcon, C.; Pennadam, S.; Alexander, C. *Chem. Soc. Rev.* **2005**, *34*, 276–285.
- (2) Picken, S. J. *Macromol. Symp.* **2000**, *154*, 95–104.
- (3) (a) Siegel, R. A.; Firestone, B. A. *Macromolecules* **1988**, *21*, 3254–3259. (b) Kwon, I. C.; Bae, Y. H.; Kim, S. W. *Nature* **1991**, *354*, 291–293. (c) Kontturi, K.; Mafe, S.; Manzanares, J. A.; Svarfvar, B. L.; Viinikka, P. *Macromolecules* **1996**, *29*, 5740–5746. (d) Holtz, J. H.; Asher, S. A. *Nature* **1997**, *389*, 829–832. (e) Miyata, Y.; Asami, N.; Urugami, T. *Nature* **1999**, *399*, 766–769.
- (4) Lengalova, A.; Pavlinek, V.; Saha, P.; Quadrat, O.; Stejskal, J. *Colloids Surf., A* **2003**, *227*, 1–8.
- (5) Park, J. H.; Chin, B. D.; Park, O. O. *J. Colloid Interface Sci.* **2001**, *240*, 349–354.
- (6) *Electroactive Polymers [EAP] Actuators as Artificial Muscles: Reality, Potential, and Challenges*; Bar-Cohen, Y., Ed.; SPIE: Bellingham, 2001.

- (7) Lestage, D. J.; Yu, M.; Urban, M. W. *Biomacromolecules* **2005**, *6*, 1561–1572.
- (8) Ionov, L.; Minko, S.; Stamm, M.; Gohy, J. F.; Jerome, R.; Scholl, A. *J. Am. Chem. Soc.* **2003**, *125*, 8302–8306.
- (9) Ruan, C. M.; Zeng, K. F.; Grimes, C. A. *Anal. Chim. Acta* **2003**, *497*, 123–131.
- (10) Stayton, P. S.; Shimoboji, T.; Long, C.; Chilkoti, A.; Chen, G. H.; Harris, J. M.; Hoffman, A. S. *Nature* **1995**, *378*, 472–474.
- (11) (a) Delaire, J. A.; Nakatani, K. *Chem. Rev.* **2000**, *100*, 1817–1846. (b) Hugel, T.; Holland, N. B.; Cattani, A.; Moroder, L.; Seitz, M.; Gaub, H. E. *Science* **2002**, *296*, 1103–1106. (c) Li, Y.; He, Y.; Tong, X.; Wang, X. *J. Am. Chem. Soc.* **2005**, *127*, 2402–2403.
- (12) Barker, S. L. R.; Ross, D.; Tarlov, M. J.; Gaitan, M.; Locascio, L. E. *Anal. Chem.* **2000**, *72*, 5925–5929.
- (13) (a) Kikuchi, A.; Okano, T. *Adv. Drug Delivery Rev.* **2002**, *54*, 53–77. (b) Li, S. K.; D’Emanuele, A. *J. Controlled Release* **2001**, *75*, 55–67. (c) Kost, J.; Langer, R. *Adv. Drug Delivery Rev.* **2001**, *46*, 125–148. (d) Peppas, N. *Curr. Opin. Colloid Interface Sci.* **1997**, *2*, 531–537.
- (14) (a) Ista, L. K.; Lopez, G. P. *J. Ind. Microbiol. Biotechnol.* **1998**, *20*, 121–125. (b) Cunliffe, D.; de las Heras Alarcon, C.; Peters, V.; Smith, J. R.; Alexander, C. *Langmuir* **2003**, *19*, 2888–2899. (c) Yamato, M.; Konno, C.; Utsumi, M.; Kikuchi, A.; Okano, T. *Biomaterials* **2002**, *23*, 561–567.
- (15) Hoffmann, J.; Plotner, M.; Kuckling, D.; Fischer, W. J. *Sens. Actuators, A* **1999**, *77*, 139–144.
- (16) Urry, D. W. *Biopolymers* **1998**, *47*, 167–178.
- (17) (a) Brunsveld, L.; Folmer, B. J. B.; Meijer, E. W.; Sijbesma, R. P. *Chem. Rev.* **2001**, *101*, 4071–4097. (b) Ciferri, A. *Macromol. Rapid Commun.* **2002**, *23*, 511–529. (c) *Supramolecular Polymers*, 2nd ed.; Ciferri, A., Ed.; CRC, Taylor and Francis: Boca Raton, FL, 2005.

controlled by the binding strength, stoichiometry, and kinetics of the supramolecular motif. The dynamic nature of these supramolecular polymeric materials allows external conditions to influence their behavior in a way that is not possible for traditional covalent macromolecules. For example, if an increase in temperature results in a decrease in the strength of the noncovalent interaction, depolymerization of the polymeric aggregate will occur.<sup>17</sup> Polymers based on this concept thus hold promise as stimuli-responsive materials that combine many of the attractive features of conventional polymers with properties that result from the reversibility of the noncovalent bonds between monomeric units. One of the easiest conceptual ways of accessing such systems is the placement of “sticky” noncovalent binding motifs on the chain ends of a bifunctional core unit. Consequently, the interactions between these end groups can result in self-assembly of the monomer units into supramolecular polymers in which noncovalent bonds are an integral part of the polymeric backbone.

The properties of such noncovalently bound aggregates have a strong dependence not only on their core components but also on the nature (stability and dynamics) of the supramolecular interactions, which control the self-assembly process. A wide range of noncovalent forces, from simple hydrophobic interactions<sup>18</sup> to more complex hydrogen bonding,<sup>19</sup> have been utilized to build such supramolecular polymers. Of particular interest here are metal–ligand interactions that are not only thermodynamically stable, but, depending on the metal ion and ligand used, can also be kinetically labile. Thus, simple addition of metal ions to a bis-ligand functionalized ditopic monomer should result in the self-assembly of metallo-supramolecular polymer.<sup>20,21</sup> The thermodynamic stability of the metal–ligand interactions will determine the size (or DP) of the aggregate,

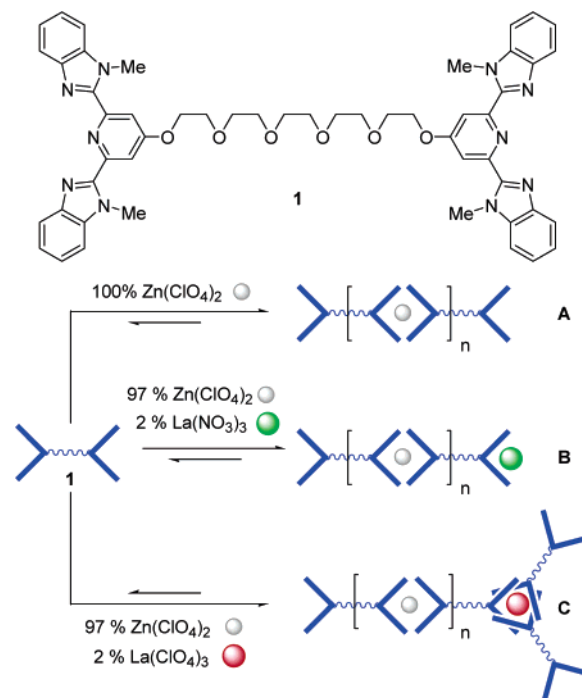


**Figure 1.** Schematic representation of the formation of metallo-supramolecular polymeric aggregates using ditopic ligand end-capped monomers with metal salts: **A**,  $\text{Zn}(\text{ClO}_4)_2$ ; **B**,  $\text{Zn}(\text{ClO}_4)_2$  and  $\text{La}(\text{NO}_3)_3$ ; and **C**,  $\text{Zn}(\text{ClO}_4)_2$  and  $\text{La}(\text{ClO}_4)_3$ , mixed with monomer **1** in acetonitrile as solvent (percentages of metal ion salts are calculated as mol % relative to **1**).

while their kinetic lability<sup>22</sup> should result in “dynamic” polymers that are in continual equilibrium and are responsive to environmental factors. Furthermore, the incorporation of metal ions opens up the possibility of imparting the functional properties of the metal ion,<sup>23</sup> for example, catalysis, light-emitting, conducting, gas binding, etc., to the resulting materials.

2,6-Bis(1'-alkylbenzimidazolyl)pyridine is a versatile terdentate ligand that has not only been shown to bind a range of metal ions, but it is also synthetically accessible in large quantities.<sup>24</sup> In addition, synthetic avenues to a range of derivatives of this ligand are known, which allows tailored functionalization of the binding unit.<sup>25</sup> Recently, some of us<sup>26</sup> have demonstrated that 2,6-bis(1'-methylbenzimidazolyl)-4-oxypyridine (O-Mebip) ligands attached to the ends of a penta(ethylene glycol) core (**1**) result in the formation of metallo-supramolecular gels<sup>27,28</sup> upon the addition of transition metal and lanthanide metal ions (Figure 1). These gels were shown to exhibit multiple stimuli-responsive behaviors, including

- (18) (a) Kastner, U. *Colloids Surf.*, **A** **2001**, *183–185*, 805–821. (b) Yao, N.; Jamieson, A. M. *Polymer* **2000**, *41*, 2925–2930. (c) Sugiyama, K.; Shiraishi, K.; Matsumoto, T. *J. Polym. Sci., Part A: Polym. Chem.* **2003**, *41*, 1992–2000.
- (19) (a) Sijbesma, R. P.; Beijer, F. H.; Brunsveld, L.; Folmer, B. J. B.; Hirscheberg, J. H. K. K.; Lange, R. F. M.; Lowe, J. K. L.; Meijer, E. W. *Science* **1997**, *278*, 1601–1604. (b) Castellano, R. K.; Rudkevich, D. M.; Rebek, J., Jr. *Proc. Natl. Acad. Sci. U.S.A.* **1997**, *94*, 7132–7137. (c) Vollmer, M. S.; Clark, T. D.; Steinem, C.; Ghadiri, M. R. *Angew. Chem., Int. Ed.* **1999**, *38*, 1598–1601. (d) Zimmerman, S. C.; Zeng, F. W.; Reichert, D. E. C.; Klotuchin, S. V. *Science* **1996**, *271*, 1095–1098. (e) Yang, X.; Hua, F.; Yamato, K.; Ruckenstein, E.; Gong, B.; Kim, W.; Ryu, C. Y. *Angew. Chem., Int. Ed.* **2004**, *43*, 6471–6474. (f) Hua, F.; Yang, X.; Gong, B.; Ruckenstein, E. *J. Polym. Sci., Part A: Polym. Chem.* **2005**, *43*, 1119–1128. (g) Lighthart, G. B. W. L.; Ohkawa, H.; Sijbesma, R. P.; Meijer, E. W. *J. Am. Chem. Soc.* **2005**, *127*, 810–811. (h) Park, T.; Zimmerman, S. C.; Nakashima, S. *J. Am. Chem. Soc.* **2005**, *127*, 6520–6521.
- (20) (a) Hinderberger, D.; Schmelz, O.; Rehahn, M.; Jeschke, G. *Angew. Chem., Int. Ed.* **2004**, *43*, 4616–4621. (b) Schmatloch, S.; van den Berg, A. M. J.; Alexeev, A. S.; Hofmeier, H.; Schubert, U. S. *Macromolecules* **2003**, *36*, 9943–9949. (c) Dobrawa, R.; Lysetska, M.; Ballester, P.; Grüne, M.; Würthner, F. *Macromolecules* **2005**, *38*, 1315–1325. (d) Kurth, D. G.; Meister, A.; Thuenemann, A. F.; Foerster, G. *Langmuir* **2003**, *19*, 4055–4057. (e) Vermonden, T.; van Steenbergen, M. J.; Besseling, N. A. M.; Marcelis, A. T. M.; Hennink, W. E.; Sudholter, E. J. R.; Cohen Stuart, M. A. *J. Am. Chem. Soc.* **2004**, *126*, 15802–15808. (f) Yount, W. C.; Juwarker, H.; Craig, S. L. *J. Am. Chem. Soc.* **2003**, *125*, 15302–15303. (g) Paulusse, J. M. J.; Sijbesma, R. P. *Angew. Chem., Int. Ed.* **2004**, *43*, 4460–4462. (h) Colombani, O.; Baroiz, C.; Bouteiller, L.; Chanéac, C.; Fromprie, L.; Lortie, F.; Montès, H. *Macromolecules* **2005**, *38*, 1752–1759. (i) Nishihara, H.; Shimura, T.; Ohkubo, A.; Matsuda, N.; Aramaki, K. *Adv. Mater.* **1993**, *5*, 752–754. (j) Constable, E. C. *Chem. Commun.* **1997**, 1073–1080. (k) Lohmeijer, B. G. G.; Schubert, U. S. *J. Polym. Sci., Part A: Polym. Chem.* **2003**, *41*, 1413–1427. (l) Schmatloch, S.; van den Berg, A. M. J.; Hofmeier, H.; Schubert, U. S. *Des. Monomers Polym.* **2004**, *7*, 191–201. (m) Hofmeier, H.; Schmatloch, S.; Wouters, D.; Schubert, U. S. *Macromol. Chem. Phys.* **2003**, *204*, 2197–2203. (n) Schubert, U. S.; Eisenbach, C. D. *Angew. Chem., Int. Ed.* **2002**, *41*, 2892–2926.
- (21) (a) Beck, J. B.; Ineman, J. M.; Rowan, S. J. *Macromolecules* **2005**, *38*, 5060–5068. (b) Iyer, P. K.; Beck, J. B.; Weder, C.; Rowan, S. J. *Chem. Commun.* **2005**, 319–320. (c) Knapton, D.; Rowan, S. J.; Weder, C. *Macromolecules* **2006**, *39*, 651–657.

- (22) (a) Yount, W. C.; Loveless, D. M.; Craig, S. L. *J. Am. Chem. Soc.* **2005**, *127*, 14488–14496. (b) Loveless, D. M.; Jeon, S. L.; Craig, S. L. *Macromolecules* **2005**, *38*, 10171–10177.
- (23) Dobrawa, R.; Würthner, F. *J. Polym. Sci., Part A: Polym. Chem.* **2005**, *43*, 4981–4995.
- (24) Piguet, C.; Buezli, J.-C. *Eur. J. Solid State Inorg. Chem.* **1996**, *33*, 165–174.
- (25) Terazzi, E.; Torelli, S.; Bernardinelli, G.; Rivera, J. P.; Benech, J.-M.; Bourgoigne, C.; Donnio, B.; Guillon, D.; Imbert, D.; Buezli, J.-C. G.; Pinto, A.; Jeannerat, D.; Piguet, C. *J. Am. Chem. Soc.* **2005**, *127*, 888–903.
- (26) (a) Beck, J. B.; Rowan, S. J. *J. Am. Chem. Soc.* **2003**, *125*, 13922–13923. (b) Zhao, Y.; Beck, J. B.; Rowan, S. J.; Jamieson, A. M. *Macromolecules* **2004**, *37*, 3529–3531. (c) Rowan, S. J.; Beck, J. B. *Faraday Discuss.* **2005**, *128*, 43–53.
- (27) Fages, F. *Angew. Chem., Int. Ed.* **2006**, *45*, 1680–1682.
- (28) For some recent examples of stimuli-responsive metallo-gels, see: (a) Kuroiwa, K.; Shibata, T.; Takada, A.; Nemoto, N.; Kimizuka, N. *J. Am. Chem. Soc.* **2004**, *126*, 2016–2021. (b) Kim, H.-J.; Zin, W.-C.; Lee, M. J. *J. Am. Chem. Soc.* **2004**, *126*, 7009–7014. (c) Kawano, S.; Fujita, N.; Shinkai, S. *J. Am. Chem. Soc.* **2004**, *126*, 8592–8593. (d) Kishimura, A.; Yamashita, T.; Aida, T. *J. Am. Chem. Soc.* **2005**, *126*, 179–183.

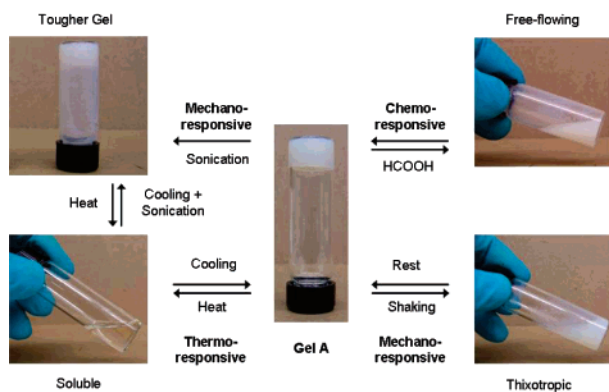


**Figure 2.** Gel A (11 wt % in acetonitrile) exhibits the typical multi-stimuli responsive behavior observed for this class of metallo-supramolecular gels.

thermo-, chemo-, and mechanical responses. The purpose of the research reported herein was to develop a better understanding of the mechanism of gel formation in these materials and subsequently to elucidate in more detail the nature of their mechano-responsive behavior.

## Results and Discussion

**Self-Assembly of Metallo-Supramolecular Gels.** Our preliminary results in this area<sup>26</sup> have shown that simple addition of an appropriate transition metal ion salt (e.g.,  $\text{Zn}(\text{ClO}_4)_2$  or  $\text{Co}(\text{ClO}_4)_2$ ) along with a small percentage of lanthanide ions (e.g.,  $\text{La}^{\text{III}}$ ,  $\text{Eu}^{\text{III}}$ ) to an acetonitrile solution of the ditopic monomer **1** results in the formation of opaque gels. Initial attempts to form gels with  $\text{Zn}(\text{ClO}_4)_2$  alone, using similar gel preparation procedures, that is, essentially heating the complex in acetonitrile until everything dissolves, and allowing to cool to room temperature, failed to yield sample spanning gels. However, further experiments show that careful control of both the heating and the cooling conditions can yield gels with **1** and  $\text{Zn}(\text{ClO}_4)_2$ . We find that, depending on the temperatures used and the concentration of the solution, gel formation can be achieved from hot, clear acetonitrile solutions of **1** and  $\text{Zn}(\text{ClO}_4)_2$  either by allowing the sample to slowly cool to ambient temperature on the bench or by quenching the sample vial in a water bath (at ambient temperature). Slowly cooled samples are much less visually homogeneous than quenched samples. This is more evident when the concentrations of the samples are reduced, heating temperature is increased, and/or cooling rate is decreased. For example, heating an 8 wt % gel to 100 °C in an oil bath, followed by either slow cooling or quenching in a water bath to ambient temperature, yields a gel-like material. However, if the sample is heated to higher temperatures and then subjected to slow cooling, the resulting material is more precipitate-like than gel-like. Thus, the behavior of these materials shows extreme sensitivity to their preparation conditions, indicative of their highly stimuli-responsive nature.

Shown in Figure 2 is gel A (11 wt % in acetonitrile), which illustrates the multi-responsive behavior typically observed in this class of gels. For example, heating results in a reversible gel–sol transition, while addition of formic acid results in the collapse of the gel. One property of particular interest is the mechano-responsive behavior. The gels formed by cooling in air exhibit pronounced thixotropic behavior. Shaking the gels results in the formation of a free-flowing liquid, which, upon standing, re-forms a turbid white gel. Interestingly, the more

the gels are shaken, the stronger the re-formed gels appear to be. This was confirmed by subjecting the gels (formed by slow cooling in air) to sonication, which results in substantially stronger gels. Gels formed by quenching in a sonication bath also appear much stronger than those formed by cooling in air. Furthermore, sonicated gels exhibit much less pronounced thixotropy, in the sense that more mechanical stress has to be applied to break the gel. However, it should be noted that the gel strength is concentration dependent and upon reducing the concentration of gels more facile thixotropy is observed. In addition, these gels over a period of a few weeks consolidate into a denser, stronger gel phase, suggesting that the initial gels are meta-stable materials.

One of the main purposes of this research was to gain a better understanding of the gel formation/mechano-responsive mechanism. In addition, we also wanted to understand the effect, if any, that addition of a small amount of lanthanide ions has on the responsive properties of the gels. While the transition metal ions form 2:1 ligand to metal ion complexes, which essentially lead to chain extension, the lanthanide ( $\text{Ln}^{\text{III}}$ ) ions, with their preference for high coordination numbers (8–10),<sup>29</sup> can potentially coordinate three O-Mebip moieties. Furthermore, utilization of  $\text{Ln}^{\text{III}}$  ions, which exhibit unusual magnetic and optical properties, opens up the possibility of using these systems to access advanced functional materials suitable for numerous applications.<sup>30</sup> Initially, lanthanide ion ( $\text{La}^{\text{III}}$  or  $\text{Eu}^{\text{III}}$ ) nitrate salts were used, and gel-like materials exhibiting multi-responsive properties were readily created.<sup>26</sup> Note, however, that the nitrate ion is coordinating in nature, and therefore its presence may compete with the O-Mebip ligand for binding sites on  $\text{Ln}^{\text{III}}$  (Figure 1B). It has been shown by Piguet, Bunzli, and co-workers<sup>30a,c</sup> that 1:1 complexes of  $\text{Ln}^{\text{III}}$  and 2,6-bis(1'-alkylbenzimidazolyl)pyridines can be prepared in which three nitrate ions are coordinated to the  $\text{Ln}^{\text{III}}$  ion. On the other hand, when lanthanide perchlorate is used, the same group showed that 3:1 complexes of 2,6-bis(1'-alkylbenzimidazolyl)pyridines and  $\text{Ln}^{\text{III}}$  are readily prepared with high yields.<sup>30b,f</sup> Thus, there is the possibility that the use of  $\text{Ln}(\text{ClO}_4)_3$  salts could result in a certain amount of branching or cross-linking points in the self-assembled materials (Figure 1C). It, therefore, became of interest to study how the different metal salts would affect the self-assembly and as a consequence the properties of the gels. It was found that gels could be prepared from complexes of **1** with combinations of  $\text{Zn}(\text{ClO}_4)_2$ /lanthanide salts, in a mole ratio of 97%  $\text{Zn}^{\text{II}}$  and 2%  $\text{La}^{\text{III}}$  relative to **1** for both  $\text{La}(\text{NO}_3)_3$  (**B**) and  $\text{La}(\text{ClO}_4)_3$  (**C**) in acetonitrile. If 2:1 and 3:1 complexes of ligand to  $\text{Zn}^{\text{II}}$  and  $\text{La}^{\text{III}}$  ions, respectively, are assumed, then 97% of the O-Mebip can bind to  $\text{Zn}^{\text{II}}$  and 3% of the O-Mebip can bind  $\text{La}^{\text{III}}$ . Of course it should be noted that in such materials it is likely that not all of the ligands will be bound and, in fact, in the case of **B** at least 2% unbound ligand will almost certainly be present, on account of the competitive binding of the nitrate

(29) Piguet, C.; Bunzli, J. G.; Bernardinelli, G.; Hopfgartner, G.; Williams, A. F. *J. Alloys Compd.* **1995**, *225*, 324–330.

(30) (a) Petoud, S.; Bunzli, J. G.; Renaud, F.; Schenk, K. J.; Piguet, C. *Inorg. Chem.* **1997**, *36*, 1345–1353. (b) Petoud, S.; Bunzli, J. G.; Renaud, F.; Piguet, C.; Schenk, K. J.; Hopfgartner, G. *Inorg. Chem.* **1997**, *36*, 5750–5760. (c) Nozary, H.; Piguet, C.; Tissot, P.; Bernardinelli, G.; Bunzli, J. G.; Deschenaux, R.; Guillon, D. *J. Am. Chem. Soc.* **1998**, *120*, 12274–12288. (d) Muller, G.; Riehl, J. P.; Schenk, K. J.; Hopfgartner, G.; Piguet, C.; Bunzli, J. G. *Eur. J. Inorg. Chem.* **2002**, 3101–3110. (e) Muller, G.; Bunzli, J. G.; Schenk, K. J.; Piguet, C.; Hopfgartner, G. *Inorg. Chem.* **2001**, *40*, 2642–2651. (f) Piguet, C.; Williams, A. F.; Bernardinelli, G.; Bunzli, J. G. *Inorg. Chem.* **1993**, *32*, 4139–4149.



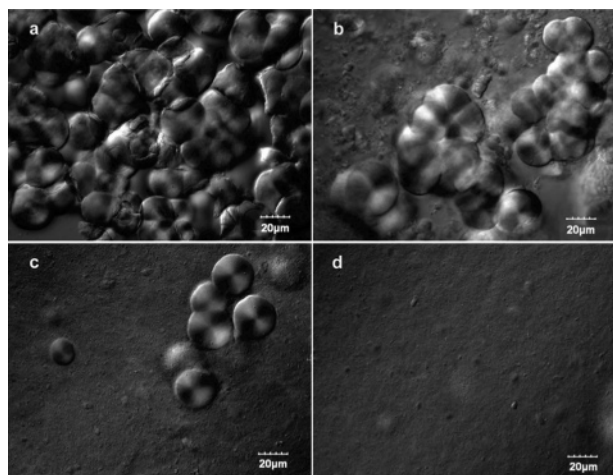


**Figure 3.** Optical microscopic images showing the effect of mechanical history on the morphology of gel A (11 wt % in acetonitrile): (a) air-cooled gel, (b) after shaking, (c) after shear at 50 Pa for 10 s, (d) after sonication for 2 min.

ions.<sup>30a,c</sup> Gels A, B, and C were therefore characterized to fully understand their behavior and gain insight into the effect that the different lanthanide salts have on the (stimuli-responsive) properties of the gels.

**Optical Microscopy of the Gels.** The self-assembly process leading to gel formation often manifests itself in the formation of characteristic microscopic morphologies.<sup>31,32</sup> As noted earlier, all three gel systems are opaque, implying a phase-separated structure. Analysis of the morphology of these phase-separated systems can provide insight into the gel formation mechanism. Laser scanning confocal microscopy indicates that a heterogeneous gel microstructure is present in all three gels formed by slow cooling under ambient conditions. A continuous particulate gel matrix is evident in the image of a freshly prepared sample of gel A (11 wt % in acetonitrile, Figure 3a). The sample consists of globular particles with an average diameter of around 20  $\mu\text{m}$ , in contact with each other, and permeated by solvent channels. The globular particles appear deformable and are able to interpenetrate at the area of contact. As discussed in the previous section, the gels exhibit pronounced mechano-responsive behavior. Microscopic examination reveals that the morphology of the gels is very sensitive to their mechanical history; that is, the structure of the globular particles present in abundance in a fresh gel can be easily destroyed by mechanical treatment. Shaking the gel results in the fracture of a significant portion of the larger micrometer-sized particles (Figure 3b). Steady shear has an even greater effect on the colloidal particles. For example, after the gel was sheared at 50 Pa for just 10 s and extracted from a rheometer cell, very few globular particles survive (Figure 3c). It is clear that when subjected to increasingly vigorous mechanical perturbation, all original globular particles disappear. Indeed, application of sonication to an existing fresh gel results in complete breakdown of the globular structure. For a gel sonicated for 2 min, most remaining particles are smaller than 5  $\mu\text{m}$  in diameter (Figure 3d). The size of the resulting particles will presumably be dependent on the soni-

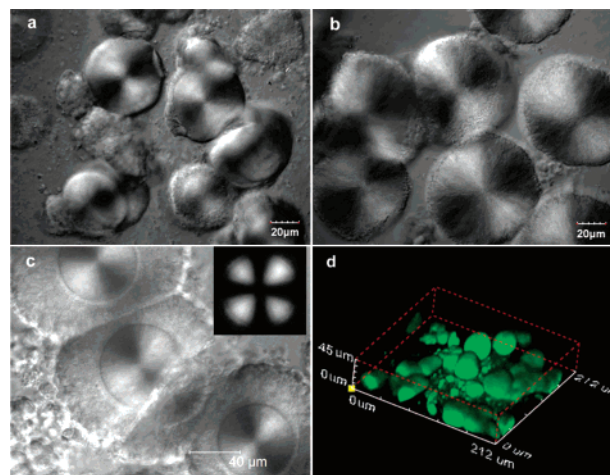


**Figure 4.** Optical microscopic images of air-cooled gels (8 wt % in acetonitrile): (a) A,  $\text{Zn}(\text{ClO}_4)_2$  only; (b) B (mole ratio  $\text{Zn}(\text{ClO}_4)_2/\text{La}(\text{NO}_3)_3 = 97/2$ ), (c) C (mole ratio  $\text{Zn}(\text{ClO}_4)_2/\text{La}(\text{ClO}_4)_3 = 97/2$ ) obtained using a laser scanning confocal microscope operated in transmitted mode. (c) Inset shows polarizing image of the gel C. (d) Laser scanning confocal microscopy (LSCM) showing 3D morphology of the globular structure in gel A (8 wt % in acetonitrile).

cation energy and time applied to the sample until a limiting value is reached.<sup>33</sup> Recalling the increased gel strength that accompanies the application of mechanical perturbation, it is evident that the broken fragments, however small, are able to re-form into an interconnecting network, even denser and more homogeneous than is present in the fresh gels. In this context, it is noted that previous studies of gels formed via adhesive interactions between colloidal particles have observed that gels formed by smaller particles have higher moduli, essentially as a consequence of the increased surface area that generates more interparticle cross-linking sites in the resulting network.<sup>34,35</sup>

From images shown in Figure 3, it is clear that the original globular morphology of the unperturbed gel cannot re-form after mechanical treatment, although the gel state is recoverable. Unfortunately, on account of the relatively fast recovery time of the gels (generally less than 30 s from visual inspection), and the fact that the first microscopy image is acquired ca. 5 min after removal of the shear, no noticeable morphology change can be observed during the gel recovery process.

The size and appearance of the globular particles in the unperturbed gels appear to differ between the three gel systems, A, B, and C. This can be seen more clearly in less concentrated samples. Figure 4 shows the images of the three gels, at 8 wt % in acetonitrile, acquired by the laser scanning confocal microscope in transmission mode. Gel A, formed without lanthanum(III) ions, has particles varying from 20 to 40  $\mu\text{m}$  in diameter (Figure 4a). The particle sizes in gel B, which contains 2 mol % lanthanum nitrate, are larger with diameters varying from 30 to 60  $\mu\text{m}$  (Figure 4b). The largest morphological difference is observed in gel C, which contains 2 mol % lanthanum perchlorate (Figure 4c). In this case, larger particles are formed, with sizes as high as 100  $\mu\text{m}$ , in which the dense core (about 40  $\mu\text{m}$ ) is surrounded by a large diffuse halo. An interesting feature of all of these gels is that they show

(31) Schneider, J. P.; Pochan, D. J.; Ozbas, B.; Rajagopal, K.; Pakstis, L.; Kretsinger, J. J. *Am. Chem. Soc.* **2002**, *124*, 15030–15037.

(32) (a) Hirst, A. R.; Smith, D. K.; Harrington, J. P. *Chem.-Eur. J.* **2005**, *11*, 6552–6559. (b) Hirst, A. R.; Smith, D. K. *Chem.-Eur. J.* **2005**, *11*, 5496–5508.

(33) Perez-Maqueda, L. A.; Duran, A.; Perez-Rodriguez, J. L. *Appl. Clay Sci.* **2005**, *28*, 245–255.

(34) Horne, D. S. *J. Chim. Phys. Phys. Chim.* **1996**, *93*, 977–986.

(35) Reddy, G. P.; Chokappa, D. K.; Naik, V. M.; Khakhar, D. V. *Langmuir* **1998**, *14*, 2541–2547.

birefringence in the core of the globular particles under polarized light, indicative of the presence of crystalline (or at least some ordered) structure. For example, polarized optical microscopy on gel **C** (Figure 4c inset) shows a well-defined spherulite texture with a distinct Maltese cross at the core of the particle, as is frequently observed in semicrystalline polymers.<sup>36,37</sup> This confirms that crystallization of the supramolecular material accompanies gelation. However, no birefringence is observed in the halo surrounding the crystalline core, indicative of a less ordered shell. The diffuse halo is not so evident in gels **A** and **B**, indicating that the volume fraction of this disordered region is greatly reduced in these two gels. It is relevant to note that in gel **C** the La<sup>III</sup> ions can bind to three O-Mebip ligands, which would result in the formation of cross-linking or branching sites in the gel, potentially inhibiting the regular stacking of the supramolecular complexes. Moreover, similar to the introduction of covalent cross-linking sites into conventional covalent polymeric materials, shorter supramolecular polymer chain length may be formed.<sup>38,39</sup> Consequently, the degree of crystallinity of the supramolecular polymer system will be diminished. A crystalline polymer is expected to exhibit higher elastic modulus and hardness than its amorphous or less crystalline counterparts.<sup>40</sup> In such circumstances, we may expect that the mechanical properties of gels containing La(ClO<sub>4</sub>)<sub>3</sub>, which are highly dependent on the elasticity of the colloidal particles,<sup>41,42</sup> may differ dramatically from those of samples without noncovalent cross-linking ions (vide infra). In addition, noting that crystallization is a thermal history-dependent process, it is expected that the size and density of the spherulite particles, and subsequent gel formation, will be highly dependent on their preparation procedures and sample concentration, as we have indeed observed.

For the less concentrated (8 wt %) samples, the particle concentrations are much lower than those of the more concentrated gels (11 wt %), and the degree of particle interpenetration is less significant. Figure 4d shows the 3D scan of gel **A** at 8 wt %, using fluorescence confocal microscopy. The figure shows that the globular particles form a three-dimensional network with large unoccupied spaces between the particles. As a consequence of mechanical perturbation during sample loading, some particles are inevitably broken, and the fragments are clearly evident in the 3D image.

**Crystallization and Particle Flocculation.** Our observation of spherulite structure from the polarized light microscopy clearly indicates that crystallization occurs during the gelation process. The XRD patterns of the three fresh gels formed in air were measured (Figure 5a). All samples show a peak at around  $2\theta = 9.36^\circ$ , corresponding to a  $d$  spacing of 0.96 nm. This peak coincides with a peak observed in the solid-state crystalline material, obtained from the crystallization of a chloroform and acetonitrile solution of **1** and Zn(ClO<sub>4</sub>)<sub>2</sub>, and presumed to arise from the packing of the 2:1 O-Mebip:Zn complexes.<sup>21a</sup> At lower angles we observe another peak, whose intensity and shape

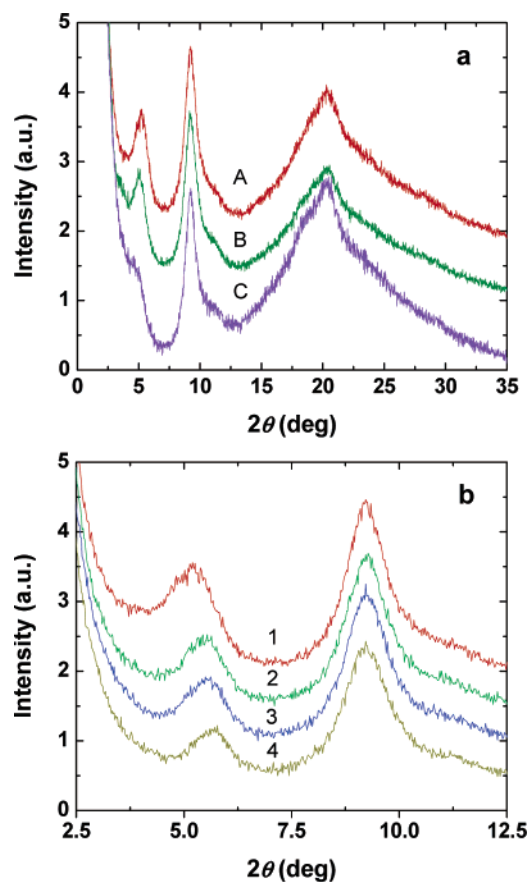


**Figure 5.** Wide-angle X-ray diffraction patterns of air-cooled gels (8 wt % in acetonitrile). (a) **A**, gel **A**; **B**, gel **B**; **C**, gel **C**. Fresh gels were directly loaded onto the sample holder, and scans were carried out immediately. (b) Gel **A** with different dryness: (1) fresh gel; (2) air-dried for 6 h; (3) air-dried for 12 h; (4) vacuum-dried for 12 h.

depend on the presence of La<sup>III</sup>. This reflection exhibits its lowest intensity for the gel containing lanthanum perchlorate (gel **C**), and similar intensity and shape for gels **A** and **B**. In addition, an amorphous halo is observed whose intensity is highest for gel **C**, suggesting that the lowest crystallinity occurs in the presence of the “cross-linking” lanthanum(III) ions. Such an interpretation is consistent with the microscopic observations where the largest diffuse halo (and therefore the smallest fraction of crystalline spherulites) is observed in gel **C** (Figure 4). Close examination shows that this low angle peak shifts to smaller  $d$  spacing with increasing drying time (Figure 5b); for example, for gel **A**, a  $d$  spacing of 1.68 nm is observed for a fresh gel sample, and the value decreases to 1.55 nm when the sample is vacuum-dried. These  $d$  spacing values are also slightly smaller than that of the low-angle peak reported previously for the same material crystallized from a chloroform and acetonitrile solvent mixture ( $d = 1.99$  nm).<sup>21a</sup> On account of its short length, the crystallization of the penta(ethylene glycol) core is not expected.<sup>43,44</sup> The solvent dependent  $d$  spacing may thus reflect the influence of the solvent on the penta(ethylene glycol) conformation in the material, and/or may indicate that solvent molecules<sup>30b,e</sup> are incorporated into the structure of crystalline **1**:Zn complexes in the gel state. In either case, the  $d$  spacings of these lower-angle peaks are consistent with expected repeat

(36) Lotz, B.; Cheng, S. Z. D. *Polymer* **2005**, *46*, 577–610.  
 (37) Gedde, U. W.; Mattozzi, A. *Adv. Polym. Sci.* **2004**, *169*, 29–73.  
 (38) Welsh, E. R.; Schauer, C. L.; Qadri, S. B.; Price, R. R. *Biomacromolecules* **2002**, *3*, 1370–1374.  
 (39) Khonakdar, H. A.; Jafari, S. H.; Taheri, M.; Wagenknecht, U.; Jehnichen, D.; Haussler, L. *J. Appl. Polym. Sci.* **2006**, *100*, 3264–3271.  
 (40) Gracias, D. H.; Somorjai, G. A. *Macromolecules* **1998**, *31*, 1269–1276.  
 (41) Macosko, C. W. *Rheology: Principles, Measurements and Applications*; VCH: New York, 1994.  
 (42) Trappe, V.; Weitz, D. A. *Phys. Rev. Lett.* **2000**, *85*, 449–452.

(43) Wu, L. M.; Lisowski, M.; Talibuddin, S.; Runt, J. *Macromolecules* **1999**, *32*, 1576–1581.  
 (44) Marentette, J. M.; Brown, G. R. *Polymer* **1998**, *39*, 1405–1414.

distances for linear aggregates, macrocycles, lamella, or even once-folded double-lamella of the **1:Zn** complex (see Supporting Information).<sup>21a,l</sup> Dilute solution viscosity measurements detect little or no significant molecular weight increase between **1** and **1:Zn** complexes, suggesting the formation of macrocycles<sup>21a,45</sup> or possibly the assembly of very small particles (vide infra) at low concentrations. It should be noted that the concentration of the gel subjected to X-ray measurements (8 wt %; or 1/15, w/v) is more than 3 times the highest concentration (1/50, w/v) of the solutions used for viscosity measurements.<sup>21a</sup> As may be expected for a crystalline material, sample preparation has a significant effect on the crystallinity of the sample. Specifically, X-ray studies on quenched samples show a decrease in intensity of the first peak and increase in intensity of the amorphous halo relative to slow cooled samples, consistent with the expectation that quenching leads to lower crystallinity.

Microscopic examinations (Figures 3 and 4) reveal that the metallo-supramolecular polymers form globular particles in the acetonitrile solvent. The gel structure can thus be considered as a volume-spanning network of semicrystalline colloidal particles dispersed in a continuous solvent medium. The data presented above suggest that, when formed either by slow cooling in air or by quenching in a sonication bath, the particles consist of an ordered core surrounded by an amorphous shell, possibly swollen by the acetonitrile solvent. Flocculation of such colloidal particles through adhesive particle–particle interactions results in the formation of a network structure, and hence gelation. Such gelation will depend on (i) the particle volume concentration and (ii) the magnitude of the particle–particle interaction energy.<sup>46</sup>

The influence of particle concentration on the properties of suspensions is best discussed in relation to the maximum packing fraction, which, as well as being controlled by the type of packing, is very sensitive to particle size distribution and particle shape.<sup>47</sup> Broad particle size distributions have higher values of maximum packing fraction because the smaller particles fit into the interstices between the larger ones. On the other hand, irregular particle shapes lead to poorer space filling and hence lower the maximum packing fraction. Particle flocculation can also lead to a low maximum packing fraction because, in general, the flocs themselves are not close-packed. The gel state or gel point, representing the minimum volume fraction necessary for a sample to form an infinite cluster, generally occurs at a very low particle volume fraction as compared to the maximum packing fraction. Various conditions such as pH, ionic strength, surfactant additives, and particle size can affect the interparticle interaction energy and thus influence the concentration at which the transition from dispersed to flocculated state occurs.<sup>48</sup>

We know that the gels in this study are formed by flocculation (or aggregation) of (semi)crystalline particles. As crystallization

is a temperature-dependent process, it is to be expected that the size and volume fraction of the spherulites (or any semicrystalline structure) will be highly dependent on the samples' thermal history. Faster cooling of the sols may lead to more crystalline particles (more nucleation sites), but with much smaller particle sizes and consequently with more amorphous structure in the systems. Slower cooling is expected to have the opposite effect. Therefore, for a system of specific weight concentration, the effective volume fraction may vary substantially, depending on the thermal history. This would explain why the formation of these gels is very sensitive to the heating and cooling rates. As most materials are more densely packed in their crystalline forms, slower cooling or annealing may result in a smaller effective volume fraction than faster cooling or quenching. Moreover, even though particles with larger sizes are obtained when a sample is cooled slowly, because the specific surface area is reduced, the overall particle–particle interaction energy is expected to decrease. Therefore, for a specified weight concentration, when a sample is heated at higher temperature and then cooled at a slower rate, the gel strength decreases, and, if the concentration is low enough, a precipitate-like, rather than gel-like, material is formed.

The primary difficulty in dealing with flocculated dispersions, both experimentally and theoretically, is the nonequilibrium nature of the gel structure. Such dispersions will macroscopically phase-separate given sufficient time.<sup>46</sup> Indeed, we observe that, under isothermal conditions, gels formed either by slow cooling or by quenching consolidate under gravity over a period of a few weeks, leaving a clear supernatant and a denser gel phase, suggesting that these systems are meta-stable. Thus, the particles within the gel network rearrange over long times, as is observed in some silica gel systems.<sup>49,50</sup> As crystallization accompanies gelation, maturing of the spherulites may also expel solvent to form denser, more ordered crystals, resulting in a smaller effective volume fraction. Such effects may be expected to influence the gel strength, and therefore all rheological studies (vide infra) were performed relatively quickly (within 24 h) after gel formation and the experimental time scales were kept relatively short (less than 3 h), to minimize any effects that are caused by changes in the metastable structure probed during the experimental lifetime.

**Dilution Behavior.** Attempts were made to measure the particle sizes of the primary dispersion particles in the sonicated gels. Such experiments are difficult, when dealing with flocculated dispersions.<sup>51,52</sup> Therefore, the 8 wt % (or 1/15, w/v) gel **A** (formed by quenching in a sonication bath) was diluted by stepwise addition of acetonitrile. It was found that, without mechanical treatment, for example, shaking or sonication, no noticeable dispersion of solvent into the gel took place overnight. With gentle shaking, a sample diluted to 1/50 (w/v) broke up into fragments, which fused together into an intact, although visually heterogeneous gel (Figure 6a). This metastable gel shows much more pronounced thixotropic behavior as compared to the mother gel, but with substantial loss of recoverable strength; that is, the more it is agitated, the weaker is the re-formed gel. After sufficient agitation, no gel re-forms, and a

(45) Chen, C.; Dormidontova, E. E. *J. Am. Chem. Soc.* **2004**, *126*, 14972–14978.

(46) Russel, W. B.; Saville, D. A.; Schowalter, W. R. *Colloidal Dispersions*; Cambridge University: Cambridge, 1989.

(47) Barnes, H. A.; Hutton, J. F.; Walters, K. *An Introduction to Rheology*; Elsevier: Amsterdam, 1989.

(48) (a) Pishvaei, M.; Graillat, C.; McKenna, T. F.; Cassagnau, P. *Polymer* **2005**, *46*, 1235–1244. (b) Burns, J. L.; Yan, Y.; Jameson, G. J.; Biggs, S. *Colloids Surf.* **2003**, *214*, 173–180. (c) Amaral, M.; Roos, A.; Asua, J. M.; Creton, C. *J. Colloid Interface Sci.* **2005**, *281*, 325–338. (d) Craciun, L.; Carreau, P. J.; Heuzey, M.; van de Ven, T.; Moan, M. *Rheol. Acta* **2003**, *42*, 410–420. (e) Guyot, A.; Chu, F.; Schneider, M.; Graillat, C.; McKenna, T. F. *Prog. Polym. Sci.* **2002**, *27*, 1573–1615.

(49) Chen, M.; Russel, W. B. *J. Colloid Interface Sci.* **1990**, *141*, 564–577.

(50) Manley, S.; Skotheim, J. M.; Mahadevan, L.; Weitz, D. A. *Phys. Rev. Lett.* **2005**, *94*, 218302-1–218302-4.

(51) Walls, H. J.; Caines, B.; Sanchez, A. M.; Khan, S. A. *J. Rheol.* **2003**, *47*, 847–868.

(52) Yziquel, F.; Carreau, P. J.; Tanguy, P. A. *Rheol. Acta* **1999**, *38*, 14–25.



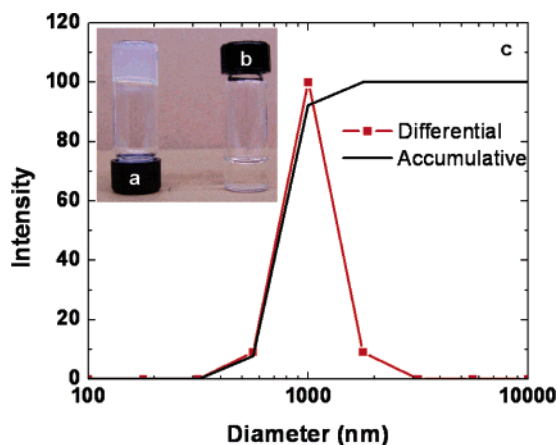


**Figure 6.** (a) A semi-opaque gel is formed by diluting gel A (8 wt %; or 1/15, w/v), formed in a sonication bath, to 1/50, w/v. (b) A clear sol is formed by further diluting the 1/50 (w/v) gel sample to 1/75, w/v. (c) Particle size and particle size distribution of the 1/75 (w/v of acetonitrile) sample of gel A. Results are derived from a CONTIN fit to the dynamic light scattering (DLS) correlation function acquired at a scattering angle of  $90^\circ$ .

dilute opaque sol results. Further dilution to 1/75 (w/v) led to immediate formation of what appears to be (from visual inspection) a clear sol (Figure 6b).

To further investigate the nature of the sol obtained through the above dilution studies, dynamic light scattering (DLS), which is a common technique to determine the hydrodynamic radius of small particles in dilute colloidal sols, was utilized. The particle sizes of gels formed by cooling in a sonication bath, as estimated from optical microscopy, are  $\sim 1 \mu\text{m}$ , near the resolution limit of the microscope. The results of DLS analysis for the dilute clear sol obtained from gel A, acquired at a scattering angle of  $90^\circ$ , are shown in Figure 6c and indicate that the dispersed particles exhibit a narrow particle size distribution, with an average particle size of around  $1.0 \mu\text{m}$ , consistent with microscopic observations. Of course it should be noted that the DLS experiments do not prove that there is complete dispersion of particles, which are prone to flocculation, and as such particle aggregates are likely to remain in the final diluted dispersion. In addition, under the high dilution conditions, some particles may partially or completely dissolve. Hence, the results should be viewed at best as an approximate representation of the characteristics of the disperse particles in the original sonicated gel.

**Electrolyte Effects.** The interactions and forces acting between dispersed particles are the key factors in determining the properties of a colloidal system.<sup>46,47</sup> Three kinds of forces should be considered in interpreting the behavior of the colloidal particles of these supramolecular materials. In addition to the usual attractive London–van der Waals' forces, and repulsive electrostatic interactions,<sup>46,47,53,54</sup> we must also consider the possibility of metal/ligand interactions. It is not unreasonable to assume that as a consequence of either incomplete binding or decomplexation processes there will always be some reactive dangling chain ends present, either on the particle surface or inside the particles. Metal/ligand binding thus potentially provides an adhesive interaction between the colloidal particles, which may contribute to flocculation. The interplay of the forces

**Table 1.** Concentrations of Formic Acid and Tetrabutylammonium Perchlorate Needed To Achieve Complete Breakdown of the Gels<sup>a</sup>

	A	B	C
HCOOH (M)	$3.49 \pm 0.17$	$3.36 \pm 0.17$	$3.56 \pm 0.17$
$\text{N}(\text{C}_4\text{H}_9)\text{ClO}_4$ (M)	$1.25 \pm 0.10$	$2.00 \pm 0.10$	$1.75 \pm 0.10$

<sup>a</sup> Gels are formed by quenching in a sonication bath with a concentration of 8 wt % or 1/15 (w/v) in acetonitrile.

acting between the suspended particles determines the flocculated structure and properties of the suspension. Of course, when considering the rheological behavior of colloidal dispersions, the Brownian (thermal) randomizing force and the viscous (hydrodynamic) forces cannot be neglected.<sup>47</sup> Therefore, considering these factors, we may expect that the gel properties, particularly the rheological behavior, can be tuned by adjusting the interparticle interactions.

Lanthanides are known to bind well to carboxylic acids.<sup>55,56</sup> Thus, addition of carboxylic acids may lead to ligand exchange and, hence, a decrease in the degree of polymerization and subsequent increase in dangling ends (more free ligands). Indeed, ligand exchange was deduced on the basis of the quenching of metal-centered emission and loss of mechanical stability, when formic acid was added to a gel containing europium nitrate.<sup>26</sup> It is noted, however, that addition of formic acid also alters the pH and ionic strength of the system, which could significantly affect the solubility of the particles and/or the stability of these colloidal gels, in which electrostatic interactions presumably exist. To explore this possibility further, formic acid was added to all three gels A, B, and C. Complete breakdown of the gels was observed for all samples, including the gel with no lanthanum(III) ions. The concentrations of formic acid needed to completely convert the gels to sols are summarized in Table 1. Within experimental error, there is essentially no difference in the concentration of formic acid required to break down all three gels. To further investigate the possibility of ligand exchange as the mechanism of the gel breakdown, formic acid titration experiments were carried out on dilute solutions of **1** and  $\text{Zn}(\text{ClO}_4)_2$  (dilute model of gel A) and of **1** and  $\text{La}(\text{ClO}_4)_3$  (with ligand-to-metal ratio of 3:1). In these studies, while decomplexation of the O-Mebip:La<sup>III</sup> complex in acetonitrile could be deduced with small amounts of formic acid (see Supporting Information), little-to-no decomplexation of the O-Mebip:Zn<sup>II</sup> complex was observed even with a very large excess (400 equiv relative to Zn<sup>II</sup>) of formic acid. The amount of formic acid required to break down the gels is about 30 mole equiv as compared to the amount of the O-Mebip ligand (ca. 60 and 900 equiv relative to Zn<sup>II</sup> and La<sup>III</sup>, respectively), which taken together with the formic acid titration data suggests that solvation or electrolyte effects play a more important role than does ligand exchange. Upon removal of the formic acid by drying the samples, and reswelling the resultant solids with acetonitrile, the gel state can be readily recovered in all three cases, confirming the chemo-responsive behavior of the gels.

To further elucidate the nature of the solvation and/or electrolyte effects, tetrabutylammonium perchlorate was added to the gels (Table 1). It was found that addition of the salt did lead to loss of gel properties in all three systems, with the lowest

(53) Shchukin, E. D.; Pertsov, A. V.; Amelina, E. A.; Zelenev, A. S. *Colloid and Surface Chemistry*; Elsevier: Amsterdam, 2001.

(54) Oosawa, F. *Polyelectrolytes*; M. Dekker: New York, 1971.

(55) Ma, L.; Evans, O. R.; Foxman, B. M.; Lin, W. *Inorg. Chem.* **1999**, *38*, 5837–5840.

(56) Kawa, M.; Frechet, J. M. J. *Chem. Mater.* **1998**, *10*, 286–296.

salt concentration required for the gel with zinc(II) alone. This may indicate a difference in the electrostatic properties of the particles containing lanthanum(III) ions. The concentrations of salt needed to break the gels are much lower than those of the formic acid, presumably reflecting the fact that formic acid is a weaker electrolyte in acetonitrile. It is noted that, in general, the concentration of salt needed to break the gels is an order of magnitude higher than that required to effectively screen polyelectrolyte interactions in aqueous solutions.<sup>46,54</sup> Because solvent is always observed to separate out from the gels immediately upon addition of salt, we infer that loss of gel properties may be a consequence of osmotic deswelling of the gel, or a salting out of the organic phase.

**Rheological Behavior.** With a better understanding of the morphology of these supramolecular gels in hand, as well as the effect the lanthanide ions have on this morphology, an examination of the mechano-behavior of the three materials was carried out. The goal here was to see if the presence of the lanthanide ions did affect the mechano-responsive behavior of the gels. As described above, gels formed by slowly cooling to room temperature exhibit very pronounced thixotropic behaviors, whereas the thixotropy of gels formed under sonication is less apparent due to their higher strength. In an attempt to ensure consistency between the different samples, the rheological studies were carried out on gels that were formed by quenching in a sonication bath. As has been shown by microscopy studies, the gel samples are sensitive to mechanical history. To optimize reproducibility and minimize the shear history effect, a meticulous procedure was followed during sample loading. All samples were subjected to an oscillatory preshear of 500% strain (applied at 5 Hz) for 30 s, and subsequently allowed to equilibrate for 90 min prior to measurements.

Oscillatory data (Figure 7a) from frequency sweeps within the linear regime indicate a highly elastic response ( $G' \gg G''$ ). The storage moduli of the three gels increase slightly with frequency over a frequency range of four decades, indicating a slightly more elastic response of the network. This behavior is typical of colloidal gels as higher deformation frequencies elicit an elastic response from local structures, which can relax at lower frequencies.<sup>42,57</sup> Gel C has elastic modulus values significantly smaller than the other two gels over the entire frequency range, while the elastic moduli of gels A and B are essentially similar. For a colloidal gel formed by flocculated particles, the yield stress has been related to the strength of the coherent network structure as the maximum force per unit area that the network can withstand before rupturing.<sup>58</sup> The yield stress can be estimated by oscillatory strain or stress measurements. Thus, the dynamic data for the three gel samples are plotted in Figure 7b as the elastic stress,  $\sigma' = G'\gamma$ , against strain. For all three gels a clear maximum is observed in the elastic stress as the strain is increased, which can be defined as the yield stress ( $\sigma_y$ ).<sup>57</sup> Gel A exhibits a value of  $\sigma_y$  ( $1893 \pm 470$  Pa) that is significantly higher than the lanthanide-containing gels, whereas gel B has a  $\sigma_y$  of  $646 \pm 198$  Pa and gel C exhibits the lowest  $\sigma_y$  value ( $242 \pm 109$  Pa). Therefore, based on these rheological studies and taken together with the morphological and XRD results, it appears that the presence of noncovalent cross-linking La<sup>III</sup> ions leads to a loss of crystallinity in these

(57) Yang, M.-C.; Scriven, L. E.; Macosko, C. W. *J. Rheol.* **1986**, *30*, 1015–1029.

(58) Nauyen, Q. D.; Boger, D. V. *J. Rheol.* **1983**, *27*, 321–349.

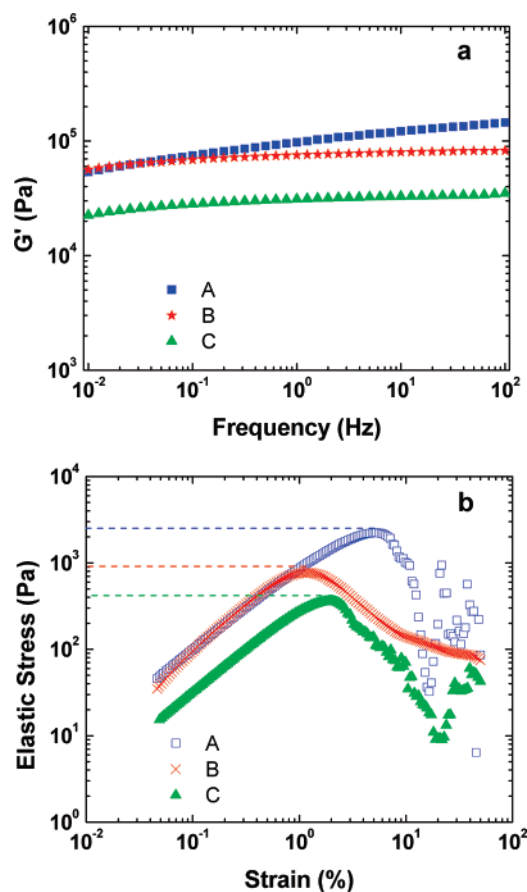


**Figure 7.** (a) Elastic modulus as a function of frequency at a strain of 0.2% for gels A, B, and C; and (b) oscillatory strain sweep data for estimating yield stress. The calculated elastic stress ( $\sigma' = G'\gamma$ ) is plotted against shear strain, and the yield point is set at where the elastic stress is maximum (dashed lines).

gels, which results in a concomitant decrease in both gel modulus and yield stress. Thus, the mechano-responsive behavior of the gels can be tailored by judicious choice of the metal ion combinations.

To quantitatively evaluate the thixotropic behavior, a shear stress loop test was applied to gel C (8 wt % in acetonitrile), and the resulting shear stress–shear rate relationship is shown in Figure 8a. The minimum stress levels during this cyclic test were maintained above 2 Pa. From Figure 8a, a yield stress can be estimated by direct extrapolation of the straight line portion of the curve to the stress axis,  $\sigma_y = 180 \pm 50$  Pa (comparable within experimental uncertainty to the value obtained from the oscillatory measurements).<sup>58</sup> It should be noted that the occurrence of wall slip between the geometry (e.g., plate) and the sample<sup>59</sup> is a common problem in concentrated colloidal systems,<sup>60–63</sup> and thus the yield stress should be considered as an approximate value. Below this critical stress value, only a limited amount of flow occurs (I), whereas when the stress is increased beyond this point the gel thins catastrophically (II). On reversing the stress, the sample

(59) Goodwin, J. W. *Rheology for Chemists: An Introduction*; Royal Society of Chemistry: Cambridge, 2000.

(60) Buscall, R.; McGowan, J. I.; Morton-Jones, A. J. *J. Rheol.* **1993**, *37*, 621–641.

(61) Russel, W. B.; Grant, M. C. *Colloids Surf., A* **2000**, *161*, 271–282.

(62) Walls, H. J.; Caines, S. B.; Sanchez, A. M.; Khan, S. A. *J. Rheol.* **2003**, *47*, 847–868.

(63) Bécu, L.; Grondin, P.; Colin, A.; Manneville, S. *Colloids Surf., A* **2004**, *263*, 146–152.



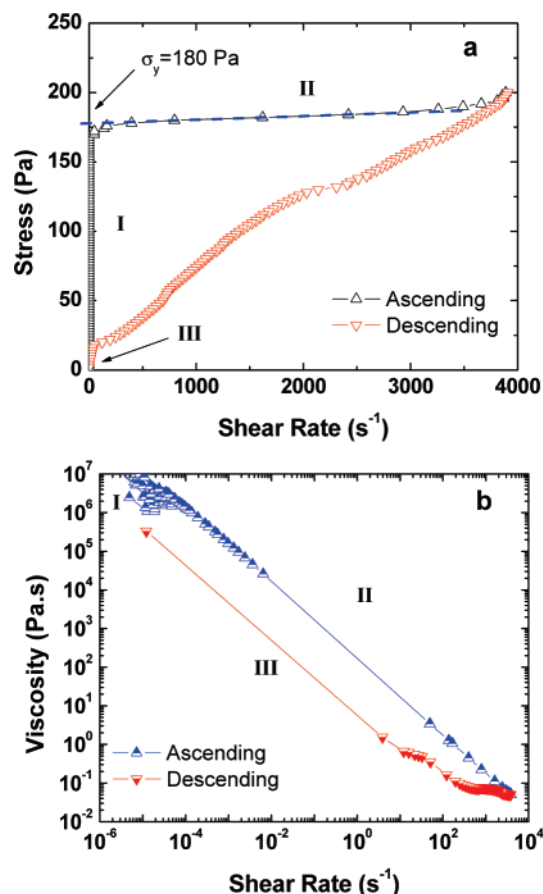


**Figure 8.** (a) Thixotropy loop shown as shear stress against shear rate, and (b) the resultant viscosity as a function of shear rate of gel **C** (8 wt % in acetonitrile), formed by quenching in a sonication bath for 5 min. Loop test was conducted by controlling stress values of 2–200–2 Pa at a step of 2 Pa per 6 s. The yield stress is indicated by an arrow in (a). Different regimes of rheological behavior are indicated (**I**, **II**, and **III**), which correspond to different proposed structures shown schematically in Figure 9; see text.

remains in the sol state until the stress reaches a comparatively low value ( $\sim 25$  Pa), at which point the gel appears to begin to re-form, as evidenced by the “step” near zero shear rate in the descending curve (**III**). The results of the thixotropy test are also plotted in the form of a viscosity–shear rate relationship in Figure 8b. As in Figure 8a, two different flow regimes can be clearly discerned in the ascending curve (**I** and **II**). In the descending curve, stage **III** can be observed more clearly with the viscosity increasing slowly at first, then more rapidly with decreasing shear rate (shear stress), apparently reflecting a transformation from the structure responsible for the thinning state back into a network architecture. Noting that a relatively long equilibration time is required for full restoration of the gel structure, the newly formed network is weaker than the original one and significantly less pronounced thixotropy is observed if a second loop test is immediately applied. If the gel network is allowed to recover for a sufficiently long time, fully restored thixotropic behavior is observed once again (see Supporting Information).<sup>64</sup>

The flow behavior of a gel formed as a consequence of flocculation may be complex.<sup>47</sup> The formation of flocs may trap part of the continuous phase, thus leading to a larger effective

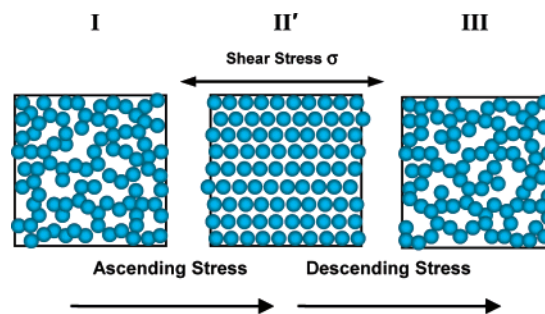


**Figure 9.** Schematic representation of possible structural changes in a metallo-supramolecular gel subjected to shear flow during the thixotropic loop test (Figure 8a). (**I**) The original structure in a gel formed by quenching in a sonication bath. The particles are not necessarily as regular as are depicted. (**II'**) Under shear flow, shear stress causes the breakdown of the interparticle bonds, and alignment of the particle occurs in the parallel to the flow, resulting in the formation of a layered structure that corresponds to the shear-thinning regime. (**III**) Re-formation of a volume-spanning structure at low shear rate during descending stress sweep.

phase volume than that of the primary particles. This produces an additional increase in the viscosity at low shear rates, above that expected from the phase volume of the individual particles. Figure 9 schematically shows the possible changes in gel structure, which occur during the thixotropic loop test. Under the application of small stress, these systems deform elastically with finite rigidity (stage **I** in Figures 8 and 9). With increasing stress, stage **I** terminates at a yield stress, above which the flocs break down into smaller aggregates and continuous deformation occurs, resulting in shear-thinning behavior. At high shear rates, a layered structure (**II'** in Figure 9) of particles in flow may be formed at which point the viscosity is then at its minimum value. If shear is terminated normally, the flow-induced layered structure will disappear gradually. In the present case, a pseudo-equilibrium state similar to that of the original gel, but with much weaker strength (see Supporting Information), begins to re-form (**III** in Figure 9) until a low stress value ( $\sim 25$  Pa) is reached. For gels that have not been sonicated and have large particle size, rupture of the particles themselves, which has been shown to occur as a consequence of the fragile nature of the colloidal particles, may be expected to contribute to the shear thinning process. Shear stress loop tests for the two stronger gels (**A** and **B**) could not be completed, as the limiting shear rate of the instrument is reached immediately after yielding.

## Conclusions

Utilizing metal–ligand binding as the driving force for the self-assembly of a ditopic ligand, which consists of a 2,6-bis-(1'-methylbenzimidazolyl)-4-oxypyridine unit attached to either end of a penta(ethylene glycol) core, we have prepared a series of three metallo-supramolecular gels in the presence of  $\text{Zn}^{\text{II}}$  alone or with a small percentage of lanthanide metal ion ( $\text{La}^{\text{III}}$ ). The resulting materials exhibit dramatic reversible responses to a variety of stimuli, including thermal, mechanical, and chemical. Microscopic examination reveals that the supramolecular metal–ligand coordination species, in acetonitrile solvent, form globular colloidal particles, which appear to exhibit spherulitic structure, indicating crystallization and phase separation accompany the gelation process. The globular particles are fragile and very sensitive to mechanical perturbation, resulting in thixotropic behavior that is highly dependent on formation history. While the gel state can be recovered after shearing, the

(64) Ferguson, J.; Kemblowski, Z. *Applied Fluid Rheology*; Elsevier: Amsterdam, 1991.

globular particles are broken into progressively smaller particles as the amount of mechanical stress is increased. This is accompanied by an increase in the strength of the resulting gel once the stress is removed. Gels formed by quenching in a sonication bath exhibit the highest strength. This is consistent with previous observations on gels formed by coagulation of adhesive spheroids and is attributed to the increase in the strength of interparticle interaction through increased surface contacts. The responsive nature of the gels can be tailored by the metal ion salts used to form the gels. For example, gels containing lanthanide salts with noncoordinating counterions (e.g., perchlorate) exhibit a lower yield stress than gels made with lanthanide salts that have competitive binding counterions (e.g., nitrate), or gels made from Zn<sup>II</sup> salts alone. This is probably a consequence of the formation of 3:1 O-Mebip:La<sup>III</sup> complexes, which result in branching or cross-linking sites and subsequently reduction in the crystallinity of the supramolecular species. When subjected to increasing shear stress, the flow characteristics of all of the gels show features reminiscent of colloidal gels, yielding followed by a shear-thinning region. It is clear that these metallo-supramolecular gels offer a facile route to multiresponsive organic/inorganic hybrid materials, whose properties can be tailored by appropriate manipulation of metal ion combinations, and taking into account the role of possible

counterion and solvent coordination. Current studies are underway to further understand the influence of pH and ionic strength on the linear and nonlinear viscoelastic behavior of these systems, as well as to understand the effects ligand structure (PEG cores with different lengths, Bip binding motifs with various substitutes, etc.), metal ion composition, and counterion have on the self-assembly process, and the consequent behavior of these gels.

**Acknowledgment.** This material is based upon work supported by the National Science Foundation under grant nos. CAREER-CHE0133164 and DMR 0513010, Polymers Program. We are grateful to Prof. Darrin Pochan and Dr. Lisa Pakstis (University of Delaware) for initial microscopy studies on these systems, Prof. Patrick Mather for use of the Anton Paar MCR 501 rheometer, Dr. Yiqiang Zhao and Dr. Jizhu Jin for invaluable discussion, and Olivier Arnoult and Dr. Kyungmin Lee for assistance with rheometric experiments.

**Supporting Information Available:** Experimental details; UV-vis titration of formic acid; gel recovery profile after a thixotropy loop test; and thixotropy loop tests. This material is available free of charge via the Internet at <http://pubs.acs.org>.

JA063408Q